IMPROVED ADAPTIVE COLOR EMBEDDING AND RECOVERY USING DC LEVEL SHIFTING

Yuko Miyashita†, Madoka Hasegawa†, Shigeo Kato† and Yuichi Tanaka‡

†Graduate School of Engineering, Utsunomiya University, 7-1-2 Yoto, Utsunomiya, Tochigi, 321-8585 Japan
‡Graduate School of BASE, Tokyo University of Agriculture and Technology, 2-24-16 Naka-cho, Koganei, Tokyo, 184-8588 Japan
Email:†11miyashita@mclaren.is.utsunomiya-u.ac.jp, {madoka, kato}@is.utsunomiya-u.ac.jp, ‡ytnk@cc.tuat.ac.jp

ABSTRACT

Several color-to-gray image mapping (CGIM) methods were proposed so far to restore a color image from its corresponding printed grayscale image. They are based on embedding chrominance values into high-frequency subbands of the luminance signal. In the conventional methods, textures often become noticeable in the chrominance-embedded gray image since subsampled chrominance values are embedded directly. As a result, qualities of the chrominance-embedded grayscale images are degraded especially for images with rich textures. In this paper, we propose an improved CGIM method using DC level shifting and directional transform. In the experimental results, our method greatly improves the qualities of both the chrominance-embedded grayscale and the restored color images in comparison with conventional methods.

Index Terms— Color restoration, color-to-gray image mapping, hybrid wavelets and directional filter banks transform, DC level shifting.

1. INTRODUCTION

In recent years, color printers are getting popular because of progress of printing technology. However, due to cost performance, monochrome printers are still frequently used for printing magazines, newspapers and so on. In such cases, color images are usually printed as grayscale images. Generally, it is impossible to restore the color image only from the printed grayscale counterpart because the color information is lost when the color image is converted into the grayscale image. Color restoration methods so called color-to-gray image mapping (CGIM) tackle the problem by embedding side information into grayscale images as a watermark [1]-[4].

Ko et al. proposed a CGIM using wavelet packet transform (WPT) [1], and de Queiroz proposed CGIM approaches using discrete wavelet transform (DWT) [2] and discrete cosine transform (DCT) [3]. In their methods, the luminance signal is decomposed into multiple subbands, and some high-frequency components are replaced with subsampled chrominance signals. As a result, a new grayscale image that contains chrominance information in order to restore the original color image is yielded after the inverse transform. However, in [1] and [2], since the transforms are separable filter banks, images with a lot of diagonal lines and edges cannot be transformed and restored effectively. Furthermore, in [3], blocking artifacts occur in the reconstructed color image because of the block-based nature of DCT. Additionally, in all methods, chrominance signals are always embedded in the high-frequency subbands at fixed positions. As a result, qualities of the chrominance-embedded grayscale images and the restored color images are often degraded.

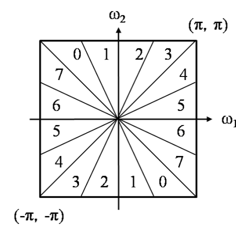

Fig. 1. Eight-band directional partitioning with $l = 3$.

To solve these problems, we proposed a CGIM method in [4] using a hybrid wavelets and directional filter banks (HWD) transform [6]. By using HWD transform, the image is decomposed into several subbands with a consideration of directionality. In contrast to the other approaches, the target subbands for embedding chrominance signals are adaptively selected. However, there still exists a room to improve the qualities of the grayscale and the restored color images.

In this paper, we proposed an improved adaptive CGIM method using DC level shifting of the chrominance signal. In the experimental results, qualities of both the chrominance-embedded grayscale images and the restored color images are greatly improved.

2. REVIEW

2.1. Hybrid Wavelets and Directional Filter Banks

2.1.1. Directional Filter Banks

Bamberger and Smith introduced directional filter banks (DFB) using quincunx and parallelogram filter banks [7] and then their improved version was developed using the efficient tree structure by Park et al. [8]. In an l-level DFB, the spectral region is divided into 2^l wedge-shaped subbands. An example of its frequency-plane partition is represented in Fig. 1. The overall sampling matrices have the following diagonal forms:

$$D_p^{(l)} = \begin{cases} diag(2^{l-1}, 2) & 1 \leq p \leq 2^{l-1} \\ diag(2, 2^{l-1}) & 2^{l-1} < p \leq 2^l \end{cases} \quad (1)$$

where p is the subband index. This means sampling is separable and all subbands have rectangular shapes.

2.1.2. HWD Transform

In DWT, an image is decomposed into subbands of high and low frequency components, and the LL subband is filtered recursively

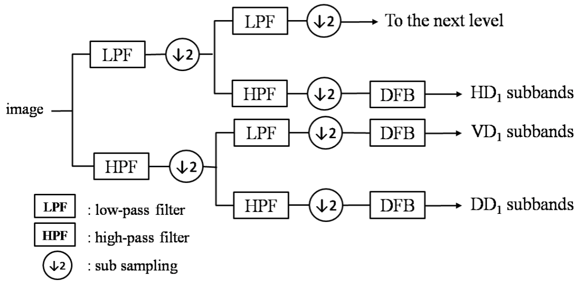

(a) HWD transform decomposition.

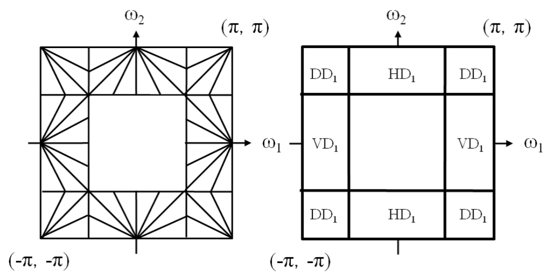

(b) Frequency partitioning.

Fig. 2. Structure of the HWD transform.

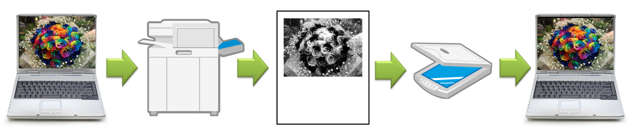

Fig. 3. CGIM model.

[5]. In HWD transform, at first, an image is decomposed into subbands with a J-level 2-D DWT. Then DFBs with l_q-levels are applied to all three high-frequency subbands at levels $1 \leq q \leq J_m$. Here, the high-frequency subbands after the DFB decomposition are defined as $HD_q = \{hd_{q,0}, \cdots, hd_{q,2^{l_q}-1}\}, VD_q = \{vd_{q,0}, \cdots, vd_{q,2^{l_q}-1}\}$ and $DD_q = \{dd_{q,0}, \cdots, dd_{q,2^{l_q}-1}\}$. Furthermore, the lowest-frequency subband is defined as L. A structure of HWD transform is illustrated in Fig. 2(a). Fig. 2(b) also shows an example of the frequency partition by HWD transform for $J = 1$, $J_m = 1$ and $l_q = 3$.

3. COLOR-TO-GRAY IMAGE MAPPING

3.1. CGIM and Color Image Restoration

The main idea of CGIM is embedding chrominance signals into high-frequency components of the luminance signal [1]-[3]. Fig. 3 shows overview of CGIM model. The color image can be restored from the printed and scanned gray image by using the embedded chrominance information. Therefore, CGIM methods can be considered as a kind of data hiding.

In CGIM, RGB signals of a color image are converted into Y, Cb, and Cr signals at the first step. Then, a subband transform is applied to the Y signal and it is decomposed into several subbands. Chrominance signals are resized to the same size of a target subband for hiding chrominance signals. They are used to replace a few subbands of the luminance signal. After the inverse transform, a new grayscale image containing color information is obtained. Hereafter, we denote the chrominance-embedded grayscale image as *textured gray image*.

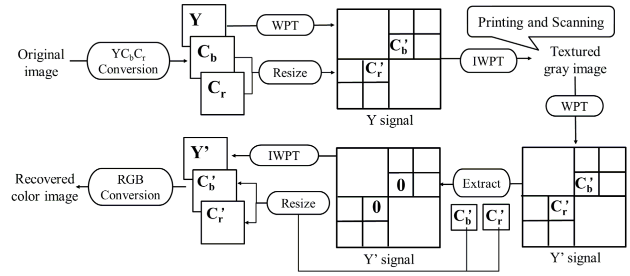

Fig. 4. WPT-based Embedding Method [1].

The method of restoring color image is based on the inverse process of the forward mapping. A textured gray image (usually it was passed through D/A and A/D conversions by a printer and a scanner, respectively) is decomposed into several subbands by the subband transform. Cb and Cr signals are then extracted from the embedded subbands used in the embedding phase. After the extraction, the subbands are replaced with zeros and the inverse transform is carried out. The extracted Cb and Cr signals are interpolated to the size of the original signals. In the last step, the obtained Y, Cb and Cr signals are converted into RGB signals. As a result, the reconstructed color image is obtained. Various transforms and target subbands are used for CGIM. In the rest of this section, we brietly review the conventional CGIM methods.

3.2. WPT-based Embedding Method

Ko et al. use two-level 2-D WPT for the subband decomposition [1]. WPT is a wavelet transform where the high-frequency subbands are transformed recursively as well as the LL subband. Thus, the n-level decomposition of WPT produces 2^{2n} subbands. Fig. 4 shows the embedding and restoring process. In the method, two subbands are replaced with subsampled Cb and Cr signals as shown in Fig. 4. The target subbands are fixed for all images.

3.3. DCT-based Embedding Method

In the method reported in [3], an $N \times N$ DCT is applied to the Y signal. The obtained high-frequency subbands are replaced with subsampled Cb and Cr signals by a zigzag scanning order. Cb and Cr signals in the block are resized from $N \times N$ to 1×1. Depending on printing and scanning environments, same chrominance signals can be embedded repeatedly. Those averages are used as the resulting chrominance signal for restoring colors.

4. ADAPTIVE COLOR-TO-GRAY IMAGE MAPPING USING DC LEVEL SHITING

In [1]-[3], only separable filters are used for the subband decomposition. However, many images have not only horizontal and vertical components, but also diagonal ones. Moreover, Cb and Cr signals are embedded in the subbands at fixed positions. To address these issues, we proposed a CGIM method using HWD transform [4] which is able to select embedding subbands adaptively. Unfortunately, similar to the conventional methods, a texture pattern would appear in the textured gray image if large chrominance values are embedded.

In this paper, we propose an improved adaptive CGIM method by shifting the chrominance signal values. Fig. 5 shows the embed-

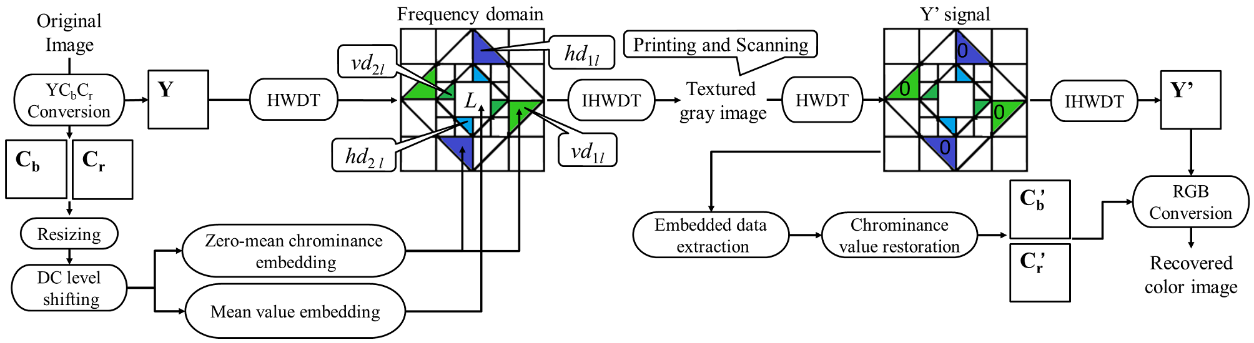

Fig. 5. Proposed process of color embedding and recovering.

ding and restoration processes of the proposed method. Instead of the direct embedding of chrominance signals in our previous CGIM, the method in this paper is composed of the following two phases:

1. Embedding zero-mean chrominance signals into high-frequency directional subbands at adaptive positions.
2. Embedding mean values of the chrominance signals repeatedly into the lowest subbands.

Indeed these mean values should be recovered as accurate as possible since they significantly affect qualities of restored color images. Hence, we embed the mean values repeatedly into the lowest subband, which can be considered as the most robust subband against D/A and A/D conversions.

4.1. Adaptive Embedding Process

The embedding process of the proposed method is basically the same as our previous method [4]. Instead of WPT or DCT, we use HWD transform as a subband transform. Furthermore, the target subbands for embedding chrominance signals are adaptively selected.

First, HWD transform with $J = 2$ and $J_m = 2$ is applied to the Y signal. Then, we choose two subbands with the lowest energies hd_{2,k_0} and vd_{2,k_1} from HD_2 and VD_2 subbands (corresponding to the second highest frequency level). The directional subband indices k_0 and k_1 are selected as follows:

$$k_0 = \arg\min_k \frac{1}{MN} \sum_{i=0}^{M-1} \sum_{j=0}^{N-1} \{hd_{2,k}(i,j)\}^2 \tag{2}$$

$$k_1 = \arg\min_k \frac{1}{MN} \sum_{i=0}^{M-1} \sum_{j=0}^{N-1} \{vd_{2,k}(i,j)\}^2 \tag{3}$$

where $k \in \{0, \cdots, 2^{l_2} - 1\}$. M and N are horizontal and vertical sizes of the subband, respectively. At the same time, each chrominance signal is subtracted its mean value to be zero-mean. Finally, in the highest frequency level, the luminance subbands hd_{1,k_0} and vd_{1,k_1} are replaced with the following $\hat{C}b$ and $\hat{C}r$ signals.

$$\overline{Cb} = \frac{1}{WH} \sum_{i=0}^{W-1} \sum_{j=0}^{H-1} Cb(i,j) \tag{4}$$

$$\overline{Cr} = \frac{1}{WH} \sum_{i=0}^{W-1} \sum_{j=0}^{H-1} Cr(i,j) \tag{5}$$

$$\hat{C}b = Cb - \overline{Cb},\ \hat{C}r = Cr - \overline{Cr} \tag{6}$$

Table 1. Embedding rule

Embedding bit	Relationship of adjacent coefficients
0	$S_L < S_R$
1	$S_L > S_R$

where W and H are the width and height of the image, respectively.

4.2. Embedding Chrominance Mean Values

As previously mentioned, the mean values of the chrominance signals are embedded as a watermark into the lowest-frequency subband. The information can be expressed in 8 bits each for Cb and Cr signals, thus the embedding information is 16 bits in total. To enhance the robustness against D/A and A/D conversions, the mean information is embedded repeatedly.

In the watermark embedding process, we use a set of adjacent coefficients $S_L = L(i, 2n-1)$ and $S_R = L(i, 2n)$ where $L(i,j)$ is the coefficient of the lowest-frequency subband. The embedding algorithm is summarized as follows:

1. *Capability Check Phase*: The difference between S_L and S_R should be small even after embedding. Therefore, the watermark is embedded if $|S_L - S_R| < T$ where T is an arbitrary threshold. Otherwise, no bit is embedded.
2. *Embedding Phase*: The signal pair passed Capability Check Phase is modified for embedding mean chrominance signals. As shown in Table 1, the values of S_L and S_R are changed as follows:

   (a) In the case of $S_L < S_R$

   Embedding '0': Values are not changed

   Embedding '1': $\begin{cases} S_L \leftarrow S_{ave} + \alpha \\ S_R \leftarrow S_{ave} - \alpha \end{cases}$

   (b) In the case of $S_L > S_R$

   Embedding '0': $\begin{cases} S_L \leftarrow S_{ave} - \alpha \\ S_R \leftarrow S_{ave} + \alpha \end{cases}$

   Embedding '1': Values are not changed

where S_{ave} is the mean value of $\boldsymbol{L}$, and α $(0 < \alpha \leq \frac{T}{2})$ is an arbitrary parameter of the embedding strength. Finally, the inverse HWD (IHWD) transform is carried out to obtain a textured gray image.

Table 2. PSNR comparison of textured gray images (dB)

	barbara	*lena*	*baboon*	*auto*
Ko et al. [1]	31.13	28.30	28.49	35.64
de Queiroz [3]	31.78	27.15	27.93	34.65
Miyashita et al. [4]	33.09	24.96	28.67	34.92
Proposed	**35.56**	**33.38**	**29.02**	**35.65**

Table 3. PSNR comparison of recovered color images (dB)

	barbara	*lena*	*baboon*	*auto*
Ko et al. [1]	33.01	**35.09**	27.00	**35.77**
de Queiroz [3]	35.41	34.33	26.87	35.15
Miyashita et al. [4]	**35.95**	34.98	**27.14**	35.62
Proposed	35.94	34.97	**27.14**	35.59

4.3. Color Restoration Process

The color restoration process is essentially the same as [4]. First, the obtained textured gray image is divided into subbands by HWD transform, and in HD'_2 and VD'_2 subbands[1], we estimate hd'_{2,k_0} and vd'_{2,k_1} by calculating (2) and (3). Then, in HD'_1 and VD'_1 subbands, Cb and Cr signals are extracted from hd'_{1,k_0} and vd'_{1,k_1}, and the subbands are replaced with zeros. At the same time, the mean values are extracted using the embedding rule from the lowest-frequency subband. Extracted information is determined by majority decision. The restored Y signal is obtained after IHWD transform is carried out. Additionally, chrominance signals are restored by the extracted mean values and resized zero-mean chrominance signals. Finally, the recovered color image is obtained from the Cb and Cr signals.

5. EXPERIMENTAL RESULTS

In this paper, *barbara*, *lena*, *baboon* and *auto* (512 × 512) are used for the experiment. For the DCT-based method [3], we used 4×4 DCT and one set of chrominance signals is embedded. We perform the proposed method with $l_1 = l_2 = 2$ for HWD transform, and $T = 15$, $\alpha = 5$. That is, the same amount of Cb and Cr signals is embedded among the methods. Fig. 6 shows enlarged textured gray images of *lena*. Printing and scanning processes are not applied for these images. It is observed that the texture pattern is less visible in the proposed method than the other methods. Table 2 shows PSNRs of the textured gray images and Table 3 presents those of the recovered color images without printing and scanning processes. It is clear that PSNRs by the proposed method are almost higher than those of the conventional methods. In the textured gray image, the proposed method was the best for all test images, and there is a difference up to 8.4 dB. By using DC level shifting to chrominance signals, textured gray image quailties have been significantly improved. Moreover, in the recovered color image, there is a difference up to 3 dB between the WPT-based method and the proposed method. The proposed method is better than the DCT-based one and comparable to our previous method in spite of its better performance on textured gray images.

For the printed and scanned versions, we used *barbara* and *lena*. In this experiment, we used an ink-jet printer EPSON PX-5V and a scanner EPSON GT-X970. All textured gray images were scaled and printed with 5760×1440 dpi, and they were scanned with 300 dpi. Table 4 shows the comparison of PSNRs after printing and scanning. They are calculated between the original Y signal and the scanned textured gray image, and between the original color image and the recovered color image. It is clear that our proposed method is the best among the methods even after printing and scanning.

[1] $(\cdot)'$ means the processed and scanned signals.

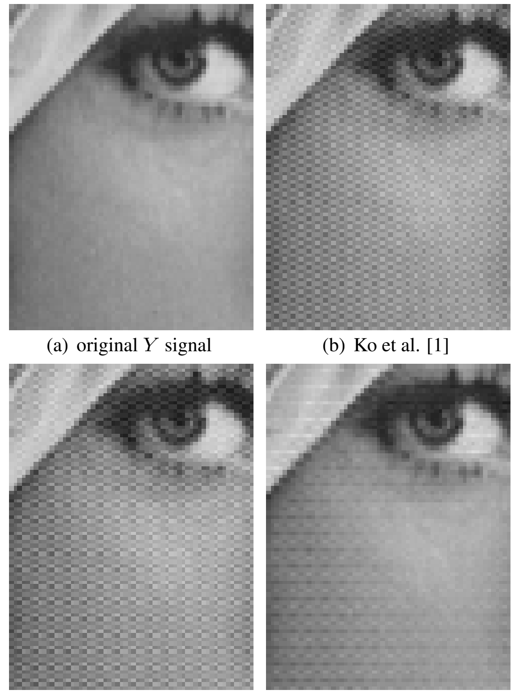

(a) original Y signal (b) Ko et al. [1]

(c) de Queiroz [3] (d) proposed

Fig. 6. Enlarged textured gray images.

Table 4. Comparison of PSNRs (dB)

	Scanned textured gray images		Recovered color images	
	barbara	*lena*	*barbara*	*lena*
Ko et al. [1]	25.82	23.50	22.20	20.73
de Queiroz [3]	20.74	23.21	18.82	20.68
Proposed	**25.98**	**24.47**	**23.31**	**23.46**

By this experiment results, even through the A/D conversion, our method was able to extract color information correctly. It is worth noting that our method estimated the embedded subbands and extracted the watermark correctly for all test images.

6. CONCLUSIONS

In this paper, we proposed an improved adaptive CGIM method using DC level shifting. The histogram of the chrominance signal is shifted to be zero-mean, and the shifted chrominance value is embedded into adaptively selected target subbands. From the experimental results, textured gray image qualities using the proposed method is superior to the existing similar methods. In addition, mean values of the chrominance signals embedded as watermark are extracted correctly from a printed and scanned textured gray image.

7. REFERENCES

[1] K.-W. Ko, O.-S. Kwon, C.-H. Son, and Y.-H. Ha, "Color embedding and recovery based on wavelet packet transform," *Journal of Imaging Science and Technology*, vol.52, no.1, pp.010501-1-010501-10, 2008.

[2] R. L. de Queiroz, K. M. Braun, "Color to gray and back: Color embedding into textured gray images," *IEEE Trans. Image Process.*, vol.15, no.6, pp.1464-1470, Jun. 2006.

[3] R. L. de Queiroz, "Reversible color-to-gray mapping using subband domain texturization," *Patt. Recog. Lett.*, vol.31, no.4, pp.269-276, Mar. 2010.

[4] Y. Miyashita, Y. Tanaka, M. Hasegawa and S. Kato, "Adaptive color-to-gray image mapping using directional transform," *Proc. International Conference on Image Processing* (*ICIP*) , pp.809-812, Oct. 2012.

[5] G. Strang and T. Q. Nguyen, *Wavelets and Filter Banks.* Boston, MA: Wellesley-Cambridge, 1996.

[6] R. Eslami and H. Radha, "A new family of nonredundant transforms using hybrid wavelets and directional filter banks," *IEEE Trans. Image Process.*, vol.16, no.4, pp.1152-1167, Apr. 2007.

[7] R. H. Bamberger and M. J. T.Smith, "A filter bank for the directional decomposition of images: Theory and design," *IEEE Trans. Signal Process.*, vol.40, no.4, pp.882-893, Apr. 1992.

[8] S. Park, M. J. T. Smith, and R. M. Mersereau, "Improved structures of maximally decimated directional filter banks for spatial image analysis," *IEEE Trans. Image Process.*, vol.13, no.11, pp.1424-1431, Nov. 2004.